CrystEngComm

RSC Publishing

PAPER

View Article Online
View Journal | View Issue

Cite this: *CrystEngComm*, 2013, **15**, 7696

Cocrystals of fisetin, luteolin and genistein with pyridinecarboxamide coformers: crystal structures, analysis of intermolecular interactions, spectral and thermal characterization†

Michał Sowa,[a] Katarzyna Ślepokura[b] and Ewa Matczak-Jon*[a]

Received 1st July 2013,
Accepted 18th July 2013

DOI: 10.1039/c3ce41285g

www.rsc.org/crystengcomm

Fisetin, luteolin and genistein, natural polyphenolic compounds of pharmaceutical interest, were combined with nicotinamide and isonicotinamide with an aim to obtain their cocrystals. A screening experiment utilizing solvent-drop grinding was conducted for those combinations. Cocrystalline phases were identified by XRPD and, as far as possible, obtained as single crystals in solution evaporation approach. Five new cocrystals were isolated, characterized by X-ray single-crystal diffraction, FT-Raman spectroscopy, thermal analysis (DSC and TG–DTA), ^{1}H NMR in solution and compared in terms of supramolecular motifs. Reported herein fisetin–nicotinamide (1 : 2) ethanol hemisolvate (**FisNam**), fisetin–isonicotinamide (1 : 1) (**FisInam**), two polymorphic forms of luteolin–isonicotinamide (1 : 1) (**LutInam**, **LutInam2**) and genistein–nicotinamide (1 : 1) monohydrate (**GenNam**) cocrystals reveal the presence of an O–H···N_{arom} heterosynthon between an O7 hydroxyl moiety of a flavonoid and the pyridyl ring of a coformer. Within those species, mutual orientations of molecules as well as flavonoid–coformer stoichiometry and solvent presence in crystal lattice are factors that imply resulting motif formation and crystal packing.

Introduction

Flavonoids comprise a vast group of naturally occurring polyphenolic compounds, considered as active pharmaceutical ingredients (APIs), and present in daily consumed vegetables, fruits and products of that origin.[1] Most of these compounds are of scientific interest due to health-prolonging effects attributed mainly to their antioxidant, antitumor and anti-inflammatory properties.[2] Some beneficial results of flavonoid administration were shown *in vivo*, yet their efficiency is hindered by low solubility in water and low bioavailability,[3,4] therefore reducing the potential of possible applications in pharmaceutical formulations or nutritional supplements. Cocrystallization, as an alternative approach to established methods for the preparation of salts, hydrates, solvates and other forms,[5,6] is a method of obtaining novel forms of active pharmaceutical ingredients (APIs) with improved physicochemical properties (*e.g.* solubility, stability, melting point) and has gained much attention in recent years. If the molecule, which forms cocrystals with the API, is ''generally regarded as safe'' for human consumption (GRAS list published by the U.S. Food and Drug Administration),[7] the cocrystal might be considered as safe for use in pharmaceutical formulations.[8] So far, cocrystallization has been successfully employed to modify the solubility of some APIs, including anticancer agents such as hexamethylenebisacetamide[9] as well as exemestane and megestrol acetate.[10] Recently, cocrystallization has been applied to improve the solubility and bioavailability of a flavonoid quercetin,[11] opening the field for improving the physicochemical properties of other compounds from this family.

This work is focused on screening pharmaceutical cocrystals of fisetin, luteolin and genistein, of which no cocrystalline forms have been reported to date. Fisetin (3,3′,4′,7-tetrahydroxyflavone) owes its research focus to its broad biological properties, including antioxidant,[12] antibacterial and antimicrobial[13] as well as anti-inflammatory action.[14,15] Some beneficial effects of fisetin administration were shown *in vivo*.[16,17] Luteolin (3′,4′,5,7-tetrahydroxyflavone) has potential as a possible antitumor agent.[18–20] Finally, genistein (4,5,7-trihydroxyisoflavone) is the most studied isoflavone and the

[a]*Department of Chemistry, Wrocław University of Technology, Wybrzeże Wyspiańskiego 27, 50-370 Wrocław, Poland. E-mail: ewa.matczak-jon@pwr.wroc.pl; Fax: +4871 320-43-60; Tel: +4871 320-41-34*

[b]*Faculty of Chemistry, University of Wrocław, 14 F. Joliot-Curie Street, 50-383 Wrocław, Poland*

† Electronic supplementary information (ESI) available: Crystallographic data tables and thermal-ellipsoid plots, FT-Raman spectra and assignments, TG–DTA and DSC plots, ^{1}H NMR spectra, Hirshfeld surfaces and 2D fingerprint plots, single-crystal images. CCDC 938495–938503. For ESI and crystallographic data in CIF or other electronic format see DOI: 10.1039/c3ce41285g

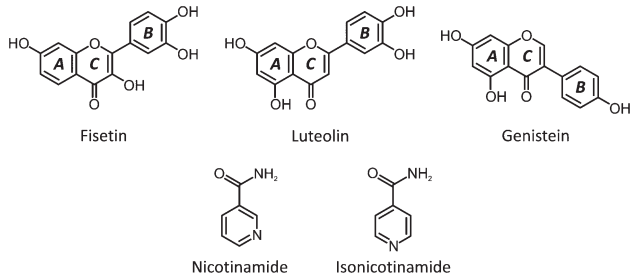

Scheme 1 Structures of flavonoids and coformers employed in this study.

predominant flavonoid in soybean enriched food. It exhibits a wide range of antitumor properties, involving influence on cell proliferation, cell cycle progression, and apoptosis.[21,22]

Suitable cocrystal formers, namely nicotinamide (Nam) and isonicotinamide (Inam), were selected based on the work of Bis *et al.*,[23] who show that the O–H···N_{arom} heterosynthon can be the most competitive motif in cocrystallizing phenolic compounds with pyridine-derived coformers, based on the analysis of structures deposited in the CSD (Cambridge Structural Database, August 2006 release).[24] Both Nam and Inam were successfully applied to cocrystallize carboxyl- and hydroxyl-derived APIs[25] including some flavonoids, such as baicalein,[26] quercetin[11] and hesperetin.[27] Scheme 1 depicts structures of flavonoids and coformers utilized in this report. Crystallization experiments resulted in five new flavonoid cocrystals suitable for X-ray single-crystal diffraction, namely fisetin–isonicotinamide (1 : 1) (**FisInam**), fisetin–nicotinamide (1 : 2) ethanol hemisolvate (**FisNam**), luteolin–isonicotinamide (1 : 1) form I (**LutInam**), luteolin–isonicotinamide (1 : 1) form II (**LutInam2**) and genistein–nicotinamide (1 : 1) monohydrate (**GenNam**). Herein we present a comparative analysis of their structures and coherent insight into essential homo- and heteromolecular interactions driving cocrystal formation. Additionally, five new materials were characterized using FT-Raman and ^{1}H NMR spectroscopy as well as thermal (TG-DTA and DSC) analysis.

Experimental

Materials

Fisetin, luteolin and genistein (all >98% HPLC) were purchased from Sino-Future Bio-Tech Co. Ltd; nicotinamide (99.5%) and isonicotinamide (99%) were obtained from Sigma-Aldrich and all of them were used as received. All solvents were purchased from POCh S.A. and used without further purification.

Screening *via* solvent-drop grinding

50 mg of flavonoid and a 1 : 1 stoichiometric amount of coformer were combined along with solvent (methanol, ethanol, ethyl acetate or water; one drop, *ca.* 25 μL) in a 5 mL stainless steel grinding jar with two 7 mm stainless steel grinding balls. Samples were ground in a Narva Vibrator Mill for 30 min (3 × 10 min with 5 min cooling periods) at a rate of 50 Hz. Resulting solids were dried overnight at ambient conditions and characterized using powder X-ray diffraction (Table 1).

Cocrystal preparation by solution evaporation (SE)‡

Fisetin–nicotinamide (1 : 2) ethanol hemisolvate (FisNam). Fisetin (25.0 mg, 0.086 mmol) and nicotinamide (150.0 mg, 1.222 mmol) were dissolved in ethyl alcohol (7 mL), with stirring at ambient temperature. The resulting solution was filtered and allowed to slowly evaporate at room temperature. Yellow plate-like crystals suitable for X-ray diffraction were harvested after 22 days (yield 58%).

Fisetin–isonicotinamide (1 : 1) (FisInam). Fisetin (25.0 mg, 0.086 mmol) and isonicotinamide (150.0 mg, 1.216 mmol) were dissolved in methyl alcohol (7 mL), with stirring at ambient temperature. The resulting solution was filtered and allowed to slowly evaporate at room temperature. Yellow block-like crystals suitable for X-ray diffraction were harvested after 4 days (yield 20%).

Luteolin–isonicotinamide (1 : 1) form I (LutInam). Luteolin (25.0 mg, 0.086 mmol) and isonicotinamide (150.0 mg, 1.216 mmol) were dissolved in an ethyl alcohol–acetone mixture (50 : 50 v/v, total 7 mL), with stirring at ambient temperature. The resulting solution was filtered and allowed to slowly evaporate at room temperature. Yellow plate-like crystals suitable for X-ray diffraction were harvested after 4 days (yield 46%).

Luteolin–isonicotinamide (1 : 1) form II (LutInam2). Luteolin (25.0 mg, 0.086 mmol) and isonicotinamide (150.0 mg, 1.216 mmol) were dissolved in isopropyl alcohol (7 mL), with stirring at ambient temperature. The resulting solution was filtered and allowed to slowly evaporate at room temperature. Yellow block-like crystals suitable for X-ray diffraction were harvested after 16 days (yield 32%).

Genistein–nicotinamide (1 : 1) monohydrate (GenNam). Genistein (25.0 mg, 0.091 mmol) and nicotinamide (150.0 mg, 1.222 mmol) were dissolved in an ethanol–methanol–water mixture (45 : 45 : 10 v/v/v, total 10 mL), with stirring at ambient temperature. The resulting solution was filtered and allowed to slowly evaporate at room temperature. Yellowish plate-like crystals suitable for X-ray diffraction were harvested after 29 days (yield 29%).

Powder diffraction analysis

X-Ray powder diffraction (XRPD) analyses were carried out on a Bruker D8-Advance diffractometer equipped with a VÅNTEC-1 detector ($\lambda_{Cu\ K\alpha1}$ = 1.5406 Å). The equipment was operated at 30 kV and 40 mA, and data were collected at room temperature in the range of 2θ = 3–40°.

Single-crystal X-ray diffraction analysis

X-Ray single crystal diffraction data for all cocrystals were collected at low temperature (100(2) or 102(2) K; details in Table S1 (ESI†)). For **FisNam**, **FisInam**, **LutInam** and **GenNam** room-temperature measurements (at 296(2) K) were also

‡ Syntheses were conducted with significant excess of the coformer to address the problem of solubility differences between the two components.

Table 1 Summary of the SDG and SE experiments

Constituents		Solvent-drop grinding/product			
		H_2O	EtOH	EtOAc	MeOH
Fisetin	Nam[e]	+[a]	✓ (**FisNam**)	+	+
	Inam	✓[b] (**FisInam**)	✓ (**FisInam**)	✓ (**FisInam**)	✓ (**FisInam**)
Luteolin	Nam	×[c]	×	×	×
	Inam	×	×	✓ (**LutInam2**)	×
Genistein	Nam	✓ (**GenNam**)	○[d]	○	○
	Inam	+	+	+	+

[a] + New cocrystalline phase, not isolated in SE experiments. [b] ✓ New cocrystalline phase, monocrystal isolated in SE experiments. [c] × Amorphous material. [d] ○ Starting materials with small quantities of new cocrystalline phase. [e] Nam: nicotinamide; Inam: isonicotinamide.

performed, details of which are presented in Tables S3 and S4, ESI.† Low-temperature data were collected on a Xcalibur R (**FisNam**, **LutInam2**, **GenNam**) or Kuma KM4-CCD (**FisInam**, **LutInam**) automated four-circle diffractometers with graphite monochromatized Mo Kα radiation, using Oxford Cryosystems coolers. Room-temperature experiments were undertaken on an Xcalibur R with Mo Kα radiation. Data collection, cell refinement, and data reduction and analysis were carried out with CRYSALISCCD and CRYSALISRED, respectively.[28] Diffraction data have been corrected for absorption effects by multi-scan.[28] Structures were solved by direct methods using SHELXS-97[29] and refined by a full-matrix least squares technique with SHELXL-2013[29] (**FisNam**, **FisInam**, **LutInam** and **LutInam2**) or SHELXL-97[29] (**GenNam**). All refinements were made with anisotropic thermal parameters for all non-H atoms (unless otherwise stated below). All H atoms were found in difference Fourier maps (except for disordered EtOH molecule in **FisNam** and catechol moiety in **LutInam2**, which were included from geometry), and in the final refinement cycles they were repositioned in their calculated positions and refined using a riding model, with C–H = 0.95 Å, N–H = 0.88 Å and O–H = 0.84 Å, and with $U_{iso}(H) = 1.2U_{eq}(C,N)$ or $1.5U_{eq}(O)$, except for water H atoms in **GenNam**, which were refined freely. During refinement of **FisNam**, the ethanol molecule was found to be disordered close to a special position (inversion center), and refined over two sites with 0.407(4) and 0.093(4) occupancies. Additionally, some geometrical restraints (SAME[29] and DFIX[29] instructions) were applied in the refinement procedure of the disordered solvent molecule. All atoms with minor occupancy were refined isotropically. For refinement of low-temperature structure of **LutInam**, the cell setting from the structure refinement at 296 K was applied, resulting in a non-reduced unit cell. In the case of **LutInam2**, one of the hydroxyl groups in the catechol moiety was found to be disordered over two positions, indicating existence of two rotameric forms of luteolin within the cocrystal. The possible presence of an impurity with three hydroxyl substituents was excluded by analyzing the luteolin sample with ESI-MS and ^{13}C NMR techniques. The disordered groups were refined with 0.904(3) and 0.096(3) occupancies and modeled with EADP[29] and EXYZ[29] constraints, which were applied to some of the catechol C atoms. All atoms with minor occupancy were refined isotropically. In the absence of significant anomalous scattering effects, Friedel pairs in **GenNam** were merged. Simulated XRPD patterns were calculated with the PowderCell 2.4 for Windows package.[30] DIAMOND[31] was used for the creation of figures.

Raman spectroscopy

Raman spectra were collected on a MultiRAM FT-Raman spectrometer (Bruker Optik GmbH, Ettlingen, Germany). Samples were scanned in the range of 3600–50 cm^{-1} with 2 cm^{-1} resolution and using a 250 mW 1064 nm laser light. Instrument control, spectra analysis and correction for fluorescence effects were performed using OPUS software (Bruker Optik GmbH, Ettlingen, Germany).

Thermal analysis

Thermogravimetric analysis (TG–DTA) was carried out using a Setaram SETSYS 16/18 thermogravimetric analyzer, operated under nitrogen atmosphere, with a heating rate of 5 °C min^{-1} and in the range of 20–400 °C (samples ~4–15 mg). Differential scanning calorimetry (DSC) measurements were performed on a Setaram DSC 92 instrument. Samples (~3–7 mg) were contained in alumina pans in the presence of air as the furnace atmosphere. Measurements were performed from ambient temperature up to 300 °C with a heating rate of 5 °C min^{-1}.

^{1}H NMR solution studies

^{1}H NMR spectra were recorded on a Bruker Avance™ 600 MHz spectrometer at 298 K. Samples were prepared by dissolving 5 mg of solid in 0.6 mL of deuterated DMSO.

Computations

Hirshfeld surface maps and 2D fingerprint plots were generated with CrystalExplorer v.3.0,[32] enabling quantitative estimation of percentage contributions for various intermolecular contacts in the reported cocrystals. Plots and calculations are presented in the ESI.†

Results and discussion

Screening experiments and crystal growth

In order to provide an insight into forms that could be possibly isolated as monocrystals *via* solution evaporation (SE) based methods, a primary screening has been conducted with the

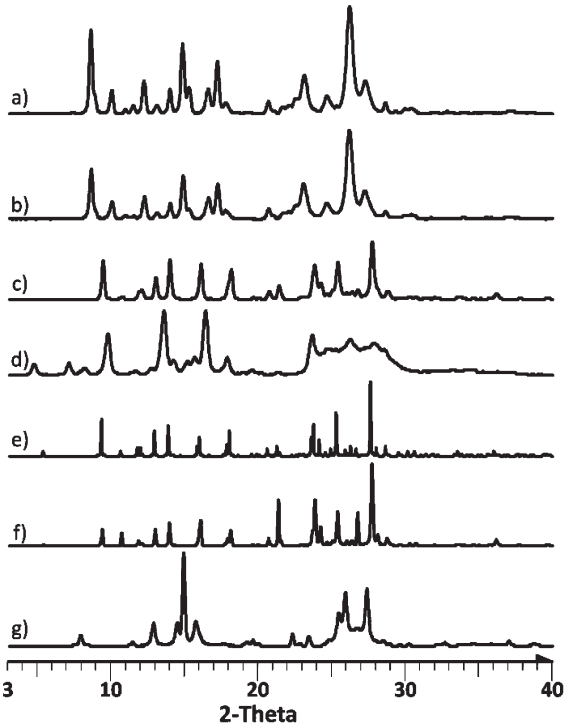

Fig. 1 XRPD patterns for fisetin–nicotinamide after grinding in a 1 : 1 stoichiometry with (a) methanol, (b) ethyl acetate, (c) ethanol, (d) H_2O and (e) pattern simulated from the single-crystal X-ray diffraction analysis of **FisNam**, (f) **FisNam** obtained by SE (ethanol), (g) a 1 : 1 physical mixture of fisetin and nicotinamide.

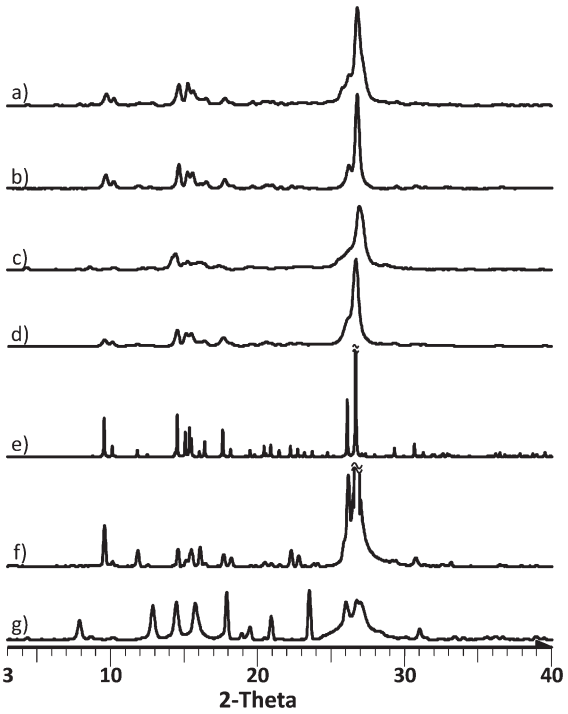

Fig. 2 XRPD patterns for fisetin–isonicotinamide after grinding in a 1 : 1 stoichiometry with: (a) methanol, (b) ethyl acetate, (c) ethanol, (d) H_2O and (e) pattern simulated from the single-crystal X-ray diffraction analysis of **FisInam**, (f) **FisInam** obtained by SE (methanol), (g) a 1 : 1 physical mixture of fisetin and isonicotinamide. Note: most intensive reflections in (f) and (g) patterns were reduced in size to improve clarity.

use of solvent-drop grinding (SDG) method.[33] Starting materials (flavonoid and coformer, either nicotinamide or isonicotinamide) were coground in 1 : 1 stoichiometric ratio with four distinct solvents (methanol, ethanol, water, ethyl acetate) yielding a total of 24 product combinations, which were subjected to XRPD analysis to identify co-crystalline materials. Solution evaporation experiments were subsequently undertaken to obtain monocrystals suitable for X-ray diffraction analysis. Within those experiments, a solvent (or solvent mixture, if one of the compounds is insoluble in pure solvent) used in a corresponding SDG procedure was employed. Results of SDG and SE experiments are outlined in Table 1.

Screening for fisetin–nicotinamide cocrystals yielded materials with three distinct powder diffraction patterns of crystalline phases different than starting materials, being the vastest result within the experiment (Fig. 1). Co-grinding with ethanol leads to a mixture of a cocrystalline phase isolated in SE experiment: the fisetin–nicotinamide (1 : 2) ethanol hemisolvate (**FisNam**) cocrystal and unreacted fisetin. Interestingly, despite 1 : 1 stoichiometry applied within screening, the 1 : 2 product is still the favored one for this combination in both SDG and SE. Two distinct XRPD patterns were observed for materials obtained by application of either H_2O or ethyl acetate and methanol. Nonetheless, application of methanol in SE experiments proved to be yet unsuccessful and no other cocrystalline forms apart from **FisNam** were isolated. Negligible solubility of fisetin in both ethyl acetate and water hinders application of pure solvents in SE experiments, moreover the use of their mixtures with solvents in which fisetin is soluble leads to either **FisNam** (for mixtures with ethanol) or powder material (for mixtures with methanol). A variety of obtained forms can be seen as a demonstration of the solvent's catalytic role in cogrinding, illustrated by changing the course of cocrystallization to different products for different solvents. On the other hand, co-grinding fisetin and isonicotinamide with H_2O, ethyl acetate, methanol or ethanol leads to the formation of only one cocrystalline phase (Fig. 2). A corresponding fisetin–isonicotinamide (1 : 1) (**FisInam**) cocrystal was isolated in SE experiments. Due to negligible solubility of fisetin in both H_2O and ethyl acetate, methanol was successfully applied as a solvent in the solution evaporation experiment, yielding monocrystals suitable for X-ray diffraction analysis. Moreover, **FisInam** could also be obtained by SE from ethanol.

Screening for luteolin cocrystals proved least successful, yielding mostly amorphous materials, except for the combination of luteolin and isonicotinamide, which leads to a diffraction pattern corresponding to non-amorphous material when ethyl acetate was applied (Fig. 3 and S41, ESI†). Pure luteolin's structure has been determined as a hemihydrate *via* X-ray diffraction analysis,[34] and as shown previously,[35] employing crystalline hydrates as reactants in SDG can lead to similar materials as if H_2O was used as a liquid for grinding. To rule out the possible interference of an additional solvent

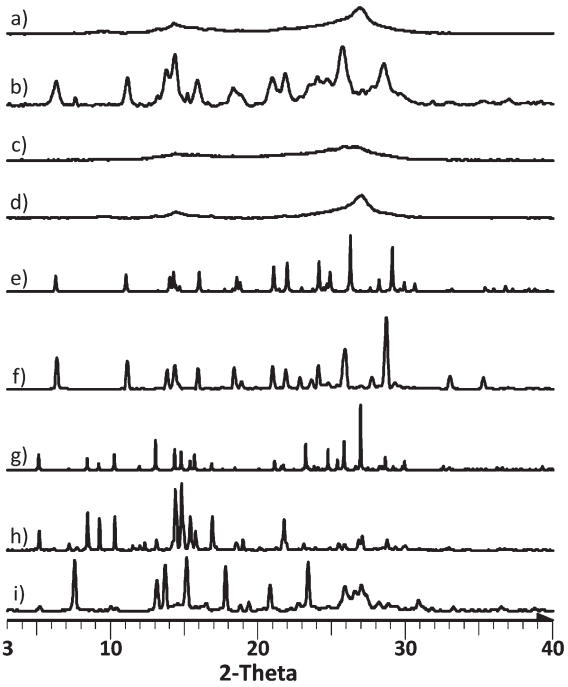

Fig. 3 XRPD patterns for luteolin–isonicotinamide after grinding in a 1 : 1 stoichiometry with: (a) methanol, (b) ethyl acetate, (c) ethanol, (d) H_2O and (e) pattern simulated from the single-crystal X-ray diffraction analysis of **LutInam2**, (f) **LutInam2** obtained by SE (2-propanol), (g) pattern simulated from the single-crystal X-ray diffraction analysis of **LutInam**, (h) **LutInam** obtained by SE (methanol–acetone (50 : 50 v/v) mixture), (i) a 1 : 1 physical mixture of luteolin and isonicotinamide.

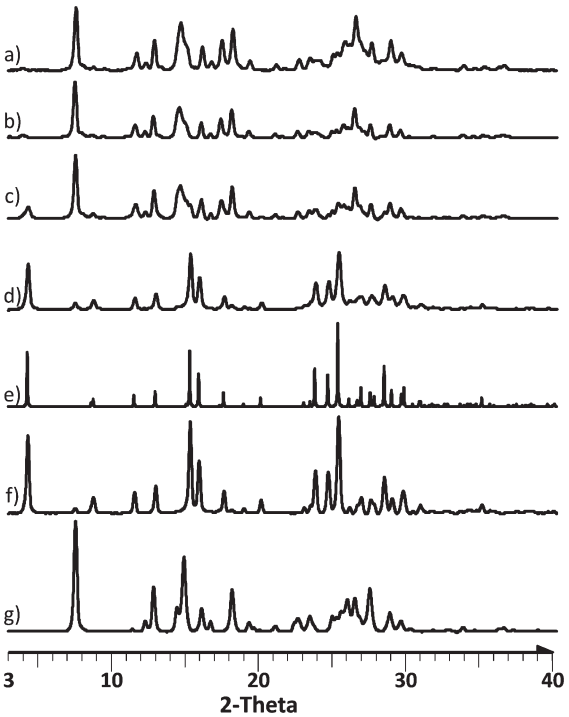

Fig. 4 XRPD patterns for genistein–nicotinamide after grinding in a 1 : 1 stoichiometry with: (a) methanol, (b) ethyl acetate, (c) ethanol, (d) H_2O and (e) pattern simulated from the single-crystal X-ray diffraction analysis of **GenNam**, (f) **GenNam** obtained by SE (methanol–ethanol–water), (g) a 1 : 1 physical mixture of genistein and nicotinamide.

(apart from the crystallization of water) neat grinding was also applied for luteolin–isonicotinamide and luteolin–nicotinamide setups, yet in both cases only amorphous materials were obtained. Similarly to other flavonoids within this report, the application of pure ethyl acetate in the SE approach is difficult due to the negligible solubility of luteolin. Solvent mixtures containing ethyl acetate were therefore applied, resulting in cocrystalline material for ethanol and methanol combinations with ethyl acetate. Alternatively, **LutInam** cocrystal could be obtained *via* SE crystallization from pure methanol and pure ethanol suggesting that ethyl acetate plays a structure-determining catalytic role only in SDG. Finally, single crystals suitable for X-ray diffraction analysis were obtained from a methanol–acetone (50 : 50 v/v) mixture, yet the **LutInam** cocrystal isolated that way provides a calculated XRPD pattern different from that observed for SDG with ethyl acetate. Surprisingly, slow evaporation of a luteolin–isonicotinamide solution in isopropyl alcohol leads to a second polymorph of the cocrystal, **LutInam2**, with a calculated diffraction pattern matching the one observed earlier for the material obtained in SDG with ethyl acetate.

Cogrinding genistein with nicotinamide and isonicotinamide leads to single crystalline phases in both cases for all employed solvents and no amorphous materials were obtained. PXRD analysis of materials obtained in genistein–nicotinamide screening shows that cogrinding both components with H_2O yields 100% conversion into a cocrystalline phase, identified in SE experiment as the genistein–nicotinamide (1 : 1) monohydrate **GenNam** cocrystal. Employing remaining solvents leads mainly to materials containing starting components (few percent conversion to **GenNam** with 99.8% ethanol and traces of cocrystalline material detected by powder diffraction when employing either ethyl acetate or methanol, Fig. 4). Full conversion into a cocrystalline phase upon cogrinding with H_2O may be explained by the presence of water molecules within the crystal lattice, while small conversion in SDG with the latter solvents might account for trace moisture presence either in samples, solvents or in the atmosphere. Although no single crystals of genistein–isonicotinamide cocrystal were isolated (which is a result not uncommon[36,37]), analysis of XRPD patterns (Fig. S42, ESI†) shows one preferred product for the four employed solvents.

Crystal structures and analysis of intermolecular interactions

Single crystals of **FisNam**, **FisInam**, **LutInam**, **LutInam2** and **GenNam** have been obtained by a solution evaporation (SE) approach. Relevant crystallographic data for cocrystals are summarized in Table S1, ESI,† whereas hydrogen bond parameters are listed in Table S2, ESI.† Packing diagrams and interactions in the reported cocrystals are presented in Fig. 5–9.

Fisetin–nicotinamide (1 : 2) ethanol hemisolvate (FisNam). The fisetin–nicotinamide (1 : 2) ethanol hemisolvate cocrystal (**FisNam**, Fig. 5) crystallizes in the $P2_1/c$ space group of the monoclinic system and contains in the asymmetric unit one

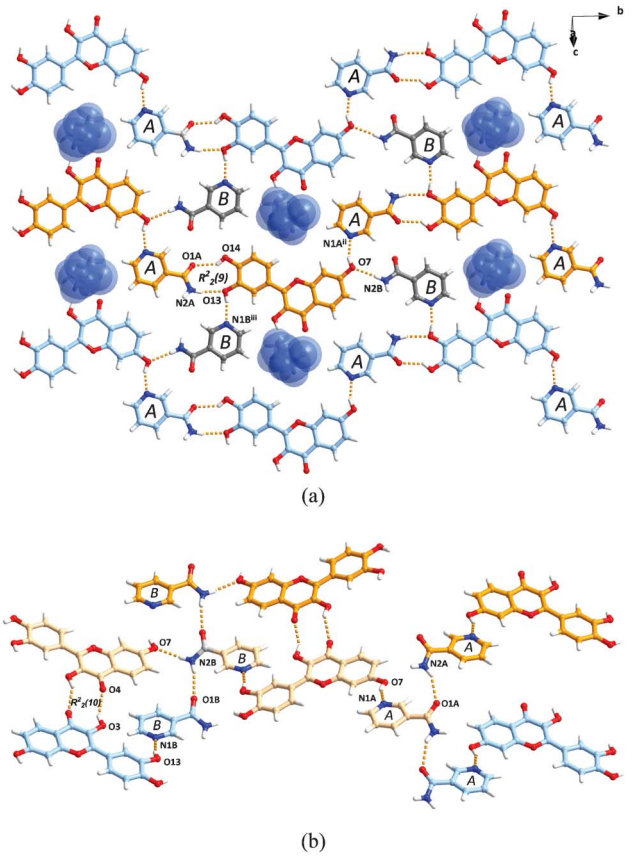

Fig. 5 Crystal packing and interactions in **FisNam**, showing (a) a 2D molecular sheet parallel to the (10$\bar{1}$) plane, assembled by neighboring Fis–NamA zig-zag tapes (blue and orange) interconnected by NamB molecules (grey), and (b) a close-up of hydrogen bond-mediated interactions between alternating, inversion-related sheets (molecular constituents of three neighboring sheets are shown in blue, tan and orange). Blue spheres represent ethanol molecules (only positions with higher occupancy factors are shown), hydrogen bonds are indicated by orange dashed lines. All symmetry codes as in Table S2, ESI† (omitted in (b)).

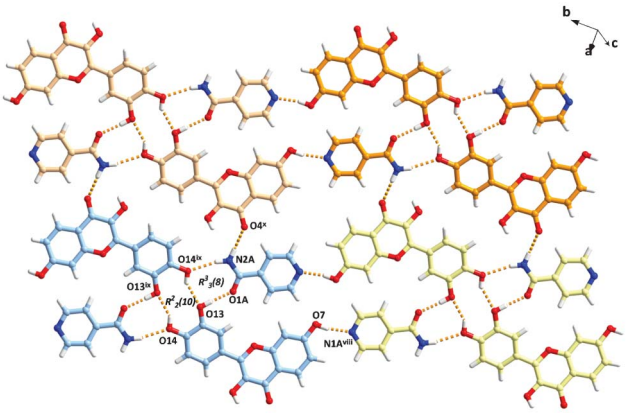

Fig. 6 Crystal packing and interactions in **FisInam**, showing a molecular layer parallel to the ($\bar{2}$12) plane, consisting of neighboring tetramers (indicated in tan, orange, blue and light-yellow). Hydrogen bonds are indicated by orange dashed lines. Symmetry codes as in Table S2, ESI.†

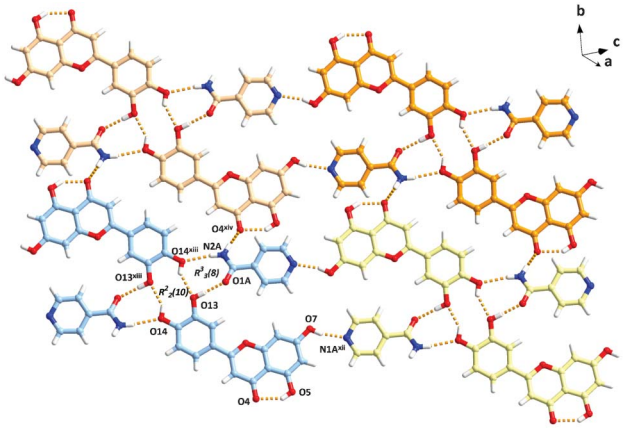

Fig. 7 Crystal packing and interactions in **LutInam**, showing a molecular layer parallel to ($\bar{1}$03), consisting of neighboring tetramers (indicated in tan, orange, blue and light-yellow). Hydrogen bonds are indicated by orange dashed lines. Symmetry codes as in Table S2, ESI.†

fisetin (Fis), two independent nicotinamide (NamA and NamB) molecules and a half of disordered ethanol molecule located close to an inversion centre (see Experimental section). Analysis of crystal packing and interactions reveals that the amide group of a NamA molecule acts with catechol moiety in the B ring of Fis through O14–H14···O1A (H···A, ∠D–H···A: 2.04 Å, 145°) and N2A–H2A1···O13 (2.03 Å, 164°) hydrogen bonds forming a hydrogen-bonded dimer with the $[R_2^2(9)]$ ring motif.[38] Similar $[R_2^2(9)]$ ring motifs involving vicinal diols and

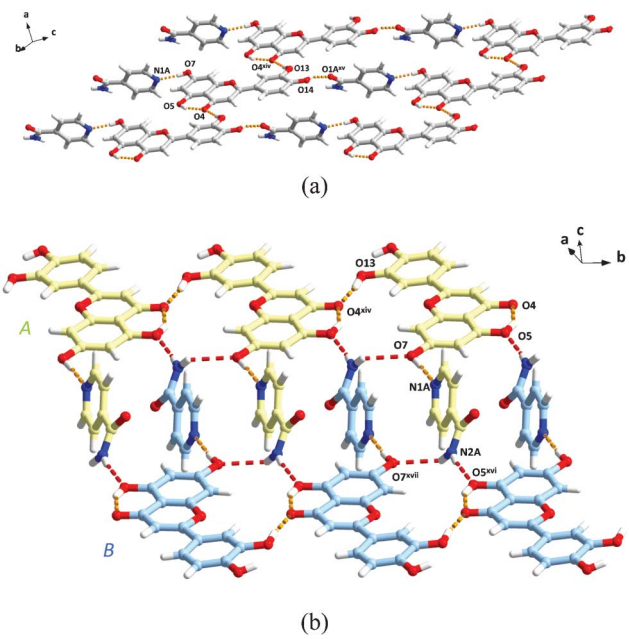

Fig. 8 Crystal packing and interactions in **LutInam2**, showing (a) formation of a sheet parallel to (101) and (b) inter-sheet interactions leading to formation of a bi-layered structure (molecular constituents of two sheets within the bi-layer are indicated in blue and light-yellow). Inter- and intra-sheet hydrogen bonding are indicated by red and orange dashed lines, respectively. Symmetry codes as in Table S2, ESI.†

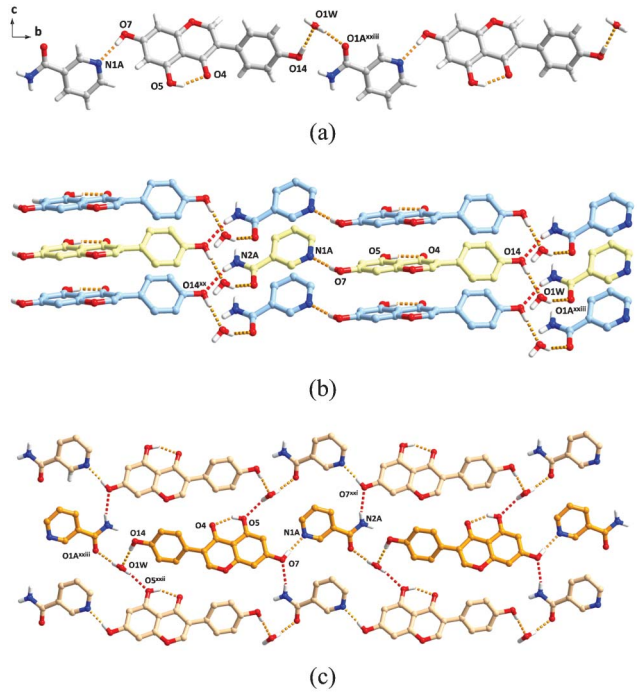

Fig. 9 Crystal packing and interactions in **GenNam**, showing (a) formation of a Gen–Nam–H_2O chain along the [110] direction, (b) inter-chain interactions leading to a stack running along *a* direction (neighboring Gen–Nam–H_2O chains are indicated in blue and light-yellow), and (c) a three dimensional network resulting from inter-stack interactions (neighboring stacks are shown in tan and orange). Intra- and inter-chain interactions are indicated by orange and red dashed lines, respectively. Symmetry codes as in Table S2, ESI.†

carboxylate moieties are observed in ascorbic acid cocrystals with betaine, sarcosine and nicotinic acid[39] as well as with L-serine,[40] but have not been reported in any so far known cocrystals of flavonoids with amide-functionalized cocrystal formers. It is also a unique feature of **FisNam** as related to the remaining cocrystals in this report. On the other hand, the amide moiety in the NamB molecule is connected with Fis through a single N2B–H2B1···O7 hydrogen bond. Within the $[R_2^2(9)]$ hydrogen-bonded dimer in **FisNam**, the planes defined by the NamA amide moiety atoms (O1A–C7A–N2A) and O14–C14–C13–O13 atoms from catechol functionality in Fis are inclined to each other with an angle of 34.5(1)°. A twist of the amide group of NamA relative to its pyridinyl ring plane is reflected in the value of the O1A–C7A–C3A–C4A torsion angle (152.2(2)°) and reveals a similar conformation to that of parent Nam crystal.[41] Adjacent Fis–NamA dimers related by the action of 2_1 screw axis are extended through O7–H7···N1A^{ii} (1.83 Å, 155°) hydrogen bonds into zig-zag tapes running along *b* direction, which are further interconnected by NamB molecules through O13–H13···N1B^{iii} (1.87 Å, 168°) and N2B–H2B1···O7 (2.03 Å, 168°) to form a sheet motif parallel to (10$\bar{1}$) plane. The dihedral angle between planes defined by the A/C rings of Fis and the N1B/C6B atoms of NamB is equal 14.9(4)°, whereas the amide group of NamB is twisted relative to its pyridyl ring plane by 29.3(2)°, as reflected in the value of the O1B–C7B–C3B–C4B torsion angle. Voids within layers are occupied by disordered ethanol molecules (Fig. 5a, see also Experimental section), hydrogen bonded to Fis molecules *via* O1E–H1E···O4 contacts (2.17 Å, 154°). On the whole, the **FisNam** cocrystal exhibits a 3D hydrogen-bonded network, in which alternating sheets are interconnected *via* three types of homomolecular hydrogen-bonded interactions. As shown in Fig. 5b, the first way comprises NamA···NamA and NamB···NamB interactions between respective amide molecules from adjacent sheets, *i.e.* N2A–H2A2···O1A^{iv} (2.14 Å, 152°) and N2B–H2B2···O1B^{v} (2.06 Å, 164°). The second route is observed in homomolecular centrosymmetric interactions between 4-oxo and 3-hydroxy functionalities of the neighboring Fis molecules, namely O3–H3···O4^{i} (2.14 Å, 152°) with a resulting $[R_2^2(10)]$ ring motif. Such homomolecular interactions between inversion-related flavonoids and utilizing the 4-oxo and neighboring 3-hydroxy moieties are encountered in pure quercetin structure[42] and its cocrystals with DABCO,[43] isonicotinic acid[27] and theobromine[44] as well as in reported herein **FisInam** cocrystal.

Fisetin–isonicotinamide (1 : 1) (FisInam). The fisetin–isonicotinamide (1 : 1) cocrystal (**FisInam**, Fig. 6) crystallizes in the $P\bar{1}$ space group of triclinic system, with one Fis and one Inam molecule in the asymmetric unit. X-Ray crystallographic analysis of **FisInam** reveals the presence of centrosymmetric tetramers assembled by Inam and Fis molecules, as illustrated in Fig. 6. Within those assemblies, O13–H13···O1A (1.78 Å, 178°), O14–H14···O13^{ix} (2.04 Å, 147°) and N2A–H2A1···O14^{ix} (2.20 Å, 166°) hydrogen bonding is observed, with resulting in-plane ring motifs that can be described by $[R_3^3(8)]$ and $[R_2^2(10)]$ graph set notations. Similar four-component assemblies are also observed in the structure of quercetin–isonicotinamide[11] and **LutInam** cocrystals, described in detail in the next paragraph. The tetrameric motif in **FisInam** is extended into a layer parallel to the ($\bar{2}$12) plane, by means of O7–H7···N1A^{viii} (1.86 Å, 169°) and N2A–H2A2···O4^{x} (2.17 Å, 154°) hydrogen bonding between Fis and Inam molecules. Planes defined by the A/C rings of fisetin and the N1A/C6A atoms of Inam are inclined over the O7–H7···N1A^{viii} hydrogen bond at a dihedral angle of 4.7(1)° (see Comparative analysis of supramolecular motifs for discussion), whereas the Inam molecule adopts a conformation similar to reported for parent compound,[45] with a O1A–C7A–C4A–C3A torsion angle of −5.1(2)°. Overall, in the crystal of **FisInam**, alternating layers are joined *via* O3–H3···O4^{vii} (1.99 Å, 161°) hydrogen bonding between inversion-related Fis molecules into a three-dimensional hydrogen-bonded network, which is additionally stabilized by π–π interactions (not discussed here).

Luteolin–isonicotinamide (1 : 1) form I (LutInam). The luteolin–isonicotinamide (1 : 1) cocrystal (**LutInam**, Fig. 7) crystallizes in the $P\bar{1}$ space group of the triclinic system, with one Lut and one Inam molecule in the asymmetric unit. Analysis of **LutInam** reveals packing and interactions similar, to some extent, to those encountered in **FisInam** as well as in a previously reported quercetin–isonicotinamide (1 : 1) cocrystal.[11] Luteolin and fisetin are isomeric compounds, with the difference reflected by the position of one hydroxyl substituent, which is present at position C3 in fisetin and at C5 in luteolin (Scheme 1). Since it is the O3 moiety, that provides stabilization of inter-layer interactions in **FisInam**, a difference between three-dimensional network arrangement and interac-

tions is to be observed in **FisInam** and **LutInam**. In luteolin structure, typically for all 5-hydroxyflavones, the O5 hydroxyl group is engaged in a strong intramolecular O5–H5···O4 (1.85 Å, 148°) hydrogen bond. Due to the fact that the C3 position remains unsubstituted and O5 is already engaged in intramolecular hydrogen bonding, the possibility to extend the structure *via* hydrogen bonding is reduced in Lut as compared to Fis. Analysis of **LutInam** reveals O13–H13···O1A (1.77 Å, 177°), O14–H14···O13^{xiii} (1.98 Å, 144°) and N2A–H2A1···O14^{xiii} (2.11 Å, 167°) hydrogen bonding between Lut and Inam molecules, leading to centrosymmetric tetramers (Fig. 7) with resulting $[R_3^3(8)]$ and $[R_2^2(10)]$ in-plane ring motifs the same as those encountered in the **FisInam** cocrystal described earlier. Tetrameric motifs are extended into a layer parallel to $(\bar{1}03)$, by means of interactions between Lut and Inam molecules, namely O7–H7···N1A^{xii} (1.86 Å, 164°) and N2A–H2A2···O4^{xiv} (2.07 Å, 155°) hydrogen bonding. The planes of A/C rings in Lut and N1A/C6A atoms in Inam are inclined over the O7–H7···N1A^{xii} interaction at a dihedral angle of 6.7(1)°, while the Inam molecule adopts a O1A–C7A–C4A–C3A torsion angle of −22.1(2)°, revealing a conformation similar to that reported for the parent compound.[45] Overall, **LutInam** exhibits a layered structure held together by hydrophobic and π–π interactions.

Luteolin–isonicotinamide (1 : 1) form II (LutInam2). The luteolin–isonicotinamide (1 : 1) cocrystal form II (**LutInam2**, Fig. 8) crystallizes in the $P\bar{1}$ space group of the triclinic system, with one Lut and one Inam molecule in the asymmetric unit. Additionally, the B ring of luteolin is disordered over two positions suggesting the presence of two rotamers within the crystal in a 0.9 : 0.1 ratio (see Experimental section). The minor rotamer is characterized by a low occupancy factor and is not involved in heteromolecular interactions, therefore being excluded from the discussion and figures. Both polymorphic forms (**LutInam** and **LutInam2**) exhibit same composition and crystallize in a common space group, yet both forms differ substantially in the aspect of intermolecular interactions and crystal packing. Polymorphism in API cocrystals is not uncommon,[46] but up to date no polymorphic flavonoid cocrystals were known. Conformation of Inam is similar in both polymorphs (O1A–C7A–C4A–C3A torsion angle values −22.1(3)° in **LutInam** and −18.2(2)° in **LutInam2**), and a slight difference in conformation of Lut is reflected in the 5.5(1)° value of the angle between its A/C and B planes in **LutInam2**. Cocrystallization typically leads to a change in the corresponding value, as seen for **LutInam** and pure luteolin[34] (9.1(1) and 2.1°, respectively). In the asymmetric unit, similar to all reported herein cocrystals, the O7 hydroxyl substituent in Lut is engaged in a O7–H7···N1A (1.86 Å, 175°) interaction with the pyridine ring of Inam, notably being the only common motif in **LutInam** and **LutInam2**. The A/C planes of Lut and N1A/C6A plane of Inam are inclined over that interaction with an angle of 74.5(1)°, being an almost perpendicular arrangement. This value is much higher than in other flavonoid cocrystals with isonicotinamide (6.7(1), 4.7(1) and 11.9(3)° for **LutInam**, **FisInam** and previously reported quercetin–isonicotinamide,[11] respectively) and is in correlation with interaction differences between the two polymorphs. Homomolecular O13–H13···O4^{xiv} (1.79 Å, 174°) contacts between neighboring Lut molecules are conserved from the pure luteolin[34] structure, with additional stabilization provided by C3–H3···O13^{xviii} (2.49 Å, 127°) weak contacts. The above mentioned interactions together with O14–H14···O1A^{xv} (2.01 Å, 146°) hydrogen bonding between Lut and Inam lead to the formation of a sheet parallel to (101) (Fig. 8a). Simultaneously, the amide moieties of Inam act as double hydrogen bond donors for N2A–H2A1···O5^{xvi} (2.05 Å, 166°) and N2A–H2A2···O7^{xvii} (2.43 Å, 135°) interactions, connecting two inversion-related sheets into a sandwich bi-layer (Fig. 8b). A three-dimensional arrangement in the crystal of **LutInam2** consists of neighboring bi-layers, held together by C–H···O (Table S2, ESI†), hydrophobic and π–π interactions.

Genistein–nicotinamide (1 : 1) monohydrate (GenNam). The genistein–nicotinamide (1 : 1) monohydrate cocrystal (**GenNam**, Fig. 9) crystallizes in the *Cc* space group of the monoclinic system. The asymmetric unit contains one genistein, one nicotinamide and one water molecule, forming a three-component molecular assembly *via* hydrogen bonding. Conformation of Gen is reflected in the angle between A/C and B planes of Gen equal 47.7(2)° and it is a value close to that reported for pure genistein[47] (53.8°) as well as its morpholine salt[48] (65.0°) and tetra-*n*-butylammonium salt[49] (50.1°). Analysis of interactions within the structure of **GenNam** reveals the presence of Gen–Nam–H_2O chains running along the [110] direction, hydrogen-boned *via* O7–H7···N1A (1.87 Å, 167°), O14–H14···O1W (1.94 Å, 177°) and O1W–H2W···O1A^{xxiii} (1.95(5) Å, 160(4)°) contacts (Fig. 9a). Within those chains, the Nam and Gen molecules are not coplanar, with a dihedral angle of 44.5(2)°, as defined between the planes of A/C rings of Gen and N1A/C6A atoms of Nam. As opposed to **FisNam**, in which the ethanol molecule does not participate in sustaining a three-dimensional hydrogen-bonded network, the water molecule in **GenNam** plays an active role in generating a one-, two- and three-dimensional network. Notably, no homomolecular hydrogen bonding is observed between Gen molecules, as well as between Nam molecules. Gen–Nam–H_2O chains are arranged in stacks running along the *a* direction, combined *via* interactions between the amide moieties of Nam and the O14 hydroxyl substituent in Gen, namely N2A–H2A1···O14^{xx} (2.10 Å, 162°) (Fig. 9b). Neighboring stacks of Gen–Nam–H_2O chains (Fig. 9c) are extended into a three-dimensional hydrogen-bonded network *via* interactions mediated by water molecules and amide moieties of Nam, namely O1W–H1W···O5^{xxii} (2.24(5), 154(4)°) and N2A–H2A2···O7^{xxi} (2.18 Å, 166°). The three-dimensional setup is additionally stabilized by an array of weak C–H···O interactions (Table S2, ESI†) as well as π–π interactions.

Comparative analysis of supramolecular motifs. To provide a coherent insight into the structure–supramolecular motif relationship for flavonoid cocrystals with pyridinecarboxamide coformers, a comparative analysis of extended structures was undertaken, taking into account their hydrogen-bonding potential, homo- and heteromolecular interactions and packing observed in five cocrystals of this study. Only O–H···O, O–H···N and N–H···O hydrogen-bonded interactions observed for flavonoids and coformers were taken into account. Recurring heteromolecular motifs are outlined on Scheme 2. Of the three analyzed flavonoids, fisetin is a compound with the vastest

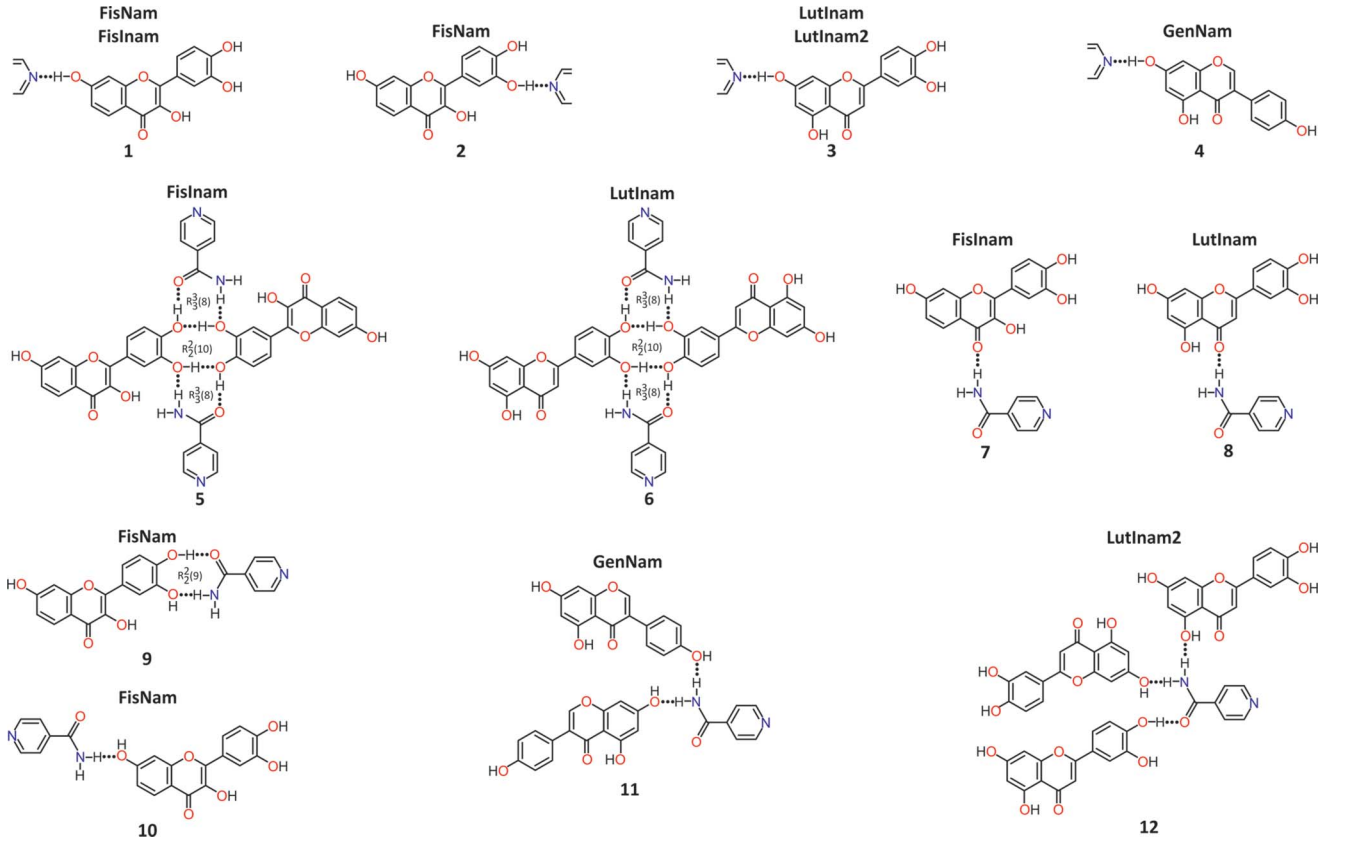

Scheme 2 Supramolecular motifs observed in **FisNam**, **FisInam**, **LutInam**, **LutInam2** and **GenNam**.

heteromolecular hydrogen-bonding potential, having four possible donor sites (Scheme 1). That potential is slightly reduced for luteolin, which despite having same amount of hydroxyl substituents as fisetin, has one hydroxyl substituent (O5) engaged in a strong intramolecular interaction (Table S2, ESI†), therefore leaving three possible H-bonding donor atoms. Finally, genistein contains only three sites with H-bonding donor potential, one of which (O5) is already engaged in intramolecular hydrogen bonding in a manner similar to that observed for luteolin (and other 5-hydroxyflavones), rendering two hydroxyl moieties attached to two distinct rings of backbone (Scheme 1).

Nam and Inam molecules reveal similar hydrogen-bonding potential, with an acceptor pyridyl N atom on one side of the molecule, and an amide moiety on the opposite, characterized by a carbonyl acceptor site and an amine donor site (Scheme 1). Despite the obvious difference between Nam and Inam resulting from structural isomerism, many similarities are observed for cocrystals with both pyridinecarboxamide coformers. Analysis of interactions shows that the dominant heterosynthon observed in all reported structures is the O–H···N_{arom} motif, utilizing the O7 hydroxyl flavonoid substituent in **FisNam** (motif 1, Scheme 2), **FisInam** (motif 1), **LutInam** (motif 3), **LutInam2** (motif 3) and **GenNam** (motif 4) as well as the O13 hydroxyl moiety as a second donor in **FisNam** (motif 2). The O–H···N_{arom} motif has been so far observed in all reported flavonoid cocrystals with pyridinecarboxamide coformers, being baicalein–nicotinamide (1 : 1),[26] quercetin–isonicotinamide (1 : 1)[11] and hesperetin–isonicotinamide (1 : 1)[27] cocrystals, which points to the robustness of this interaction for flavonoid–pyridinecarboxamide setup. Due to the O–H···N_{arom} motif similarities, it is the remaining two types of interactions, namely hydrogen-bonding in which amide moieties of Nam and Inam are engaged (correlated with mutual orientations of molecules), and flavonoid homomolecular interactions that are major factors closely related to packing observed in flavonoid cocrystals with pyridinecarboxamide coformers. Additionally, both flavonoid–coformer stoichiometry as well as solvent molecules present in the crystal lattice exhibit profound effects on analyzed relationships and therefore the 1 : 2 fisetin–nicotinamide ethanol hemisolvate (**FisNam**) and 1 : 1 genistein–nicotinamide monohydrate (**GenNam**) cocrystals are distinct as related to 1 : 1 **FisInam**, **LutInam** and **LutInam2** cocrystals so that their comparison is not straightforward.

Interestingly, in some cases, the O7 moiety (O–H···N_{arom} motif donor) acts additionally as an acceptor in the N–H···O hydrogen bond with the amide substituent of the coformer molecule. Such interactions are in correlation with the angle in which the flavonoid and pyridinecarboxamide molecules are inclined over the O–H···N_{arom} interactions. For 1 : 1 cocrystals, in which the arrangement is somewhat distant from coplanar (as defined by values of angle between A/C planes of flavonoid and the plane of coformer backbone of

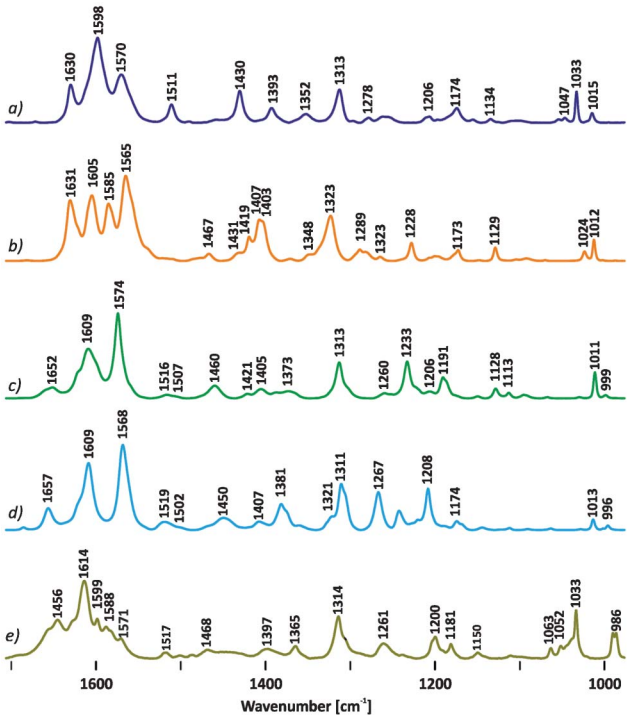

Fig. 10 Fingerprint region (1700–1000 cm^{-1}) in the FT-Raman spectra of the (a) **FisNam**, (b) **FisInam**, (c) **LutInam**, (d) **LutInam2** and (e) **GenNam** cocrystals.

44.5(2)° for **GenNam** and 74.5(1)° for **LutInam2**), the O7 substituent is simultaneously engaged in the N–H···O interaction with amide functionality of a Nam/Inam molecule (motifs 11 and 12). A close to coplanar flavonoid–coformer arrangement over the O–H···N_{arom} interaction such as in **FisInam** (4.7(1)°) and **LutInam** (6.7(1)°) cocrystals provides a steric hindrance and isolates O7 from additional interactions. Moreover, common supramolecular motifs are observed in **FisInam** and **LutInam** (motifs 5, 6, 7, 8), which lead to similar 2D layer arrangements.

Homomolecular interactions between flavonoid molecules are involved in generating two-dimensional hydrogen-bonded networks in **FisInam**, **LutInam** and **LutInam2**. Additionally, it is the O3 hydroxyl functionality in Fis that sustains the three-dimensional arrangement in **FisNam** and **FisInam** and homomolecular interactions between Lut molecules observed in **LutInam2** are conserved from the pure Lut structure.[34] The two polymorphic forms, **LutInam** and **LutInam2**, exhibit distinct interactions and crystal lattice packing with the only common supramolecular motif being the O–H···N_{arom} interaction, in which the O7 hydroxyl substituents of Lut and the pyridyl ring in Inam are engaged (motif 3). This may account for the differences in the angle at which the A/C plane of Lut and the N1A/C6A plane of Nam are inclined, which leads to four component assemblies (motif 6, Fig. 7) arranged into a layered structure in **LutInam**, as opposed to **LutInam2** (motif 12), which exhibits a distinct bi-layered structure (Fig. 8b). **FisNam**, in which two independent Nam molecules are present in the crystal lattice, is the only cocrystal herein reported, where homomolecular hydrogen-bonded interactions between coformer molecules are observed. Within those interactions, the carbonyl O1 atom and N2 amide substituents of both Nam A and Nam B are engaged in homomolecular hydrogen bonding with amide groups of neighboring Nam A and Nam B molecules, respectively, leading to molecular chains. Such an arrangement is found not only in the pure Nam structure,[41] but also in the baicalein–nicotinamide (1 : 1) cocrystal,[26] suggesting that it might be a recurring motif in flavonoid cocrystals with Nam. Worth noting is the presence of $[R_2^2(9)]$ hydrogen-bonded ring motif (motif 9), being a unique feature as compared to flavonoid cocrystals reported so far. The most distinct among the five reported cocrystals is the genistein–nicotinamide (1 : 1) monohydrate (**GenNam**) cocrystal, in which solvent molecules (water) participate in generating 1D, 2D and 3D hydrogen bonded networks. Within those interactions, water molecules act as tri-fold O–H···O hydrogen bond donors and acceptors. Apart from universal O7–H···N_{arom} interactions and N–H···O contacts between NH_2 moieties of Nam and O14 and O7 hydroxyl substituents of Gen (motif 11), no other hetero- or homomolecular interactions are observed and additional stabilization of the 3D arrangement is provided by homomolecular π–π interactions similar to those observed in **LutInam** as well as C–H···O contacts. Additional information concerning intermolecular interactions can be deduced from Hirshfeld surface analyses (plots and calculations are presented in the ESI†).

Characterization of cocrystals

The **FisNam**, **FisInam**, **LutInam**, **LutInam2** and **GenNam** cocrystals were investigated using Raman spectroscopy and thermal (TG-DTA, DSC) analysis. Moreover, samples dissolved in DMSO were subjected to ^{1}H NMR analysis, which confirmed their identity, purity and flavonoid–coformer stoichiometric ratio (see ESI† for further details). Notably, indistinguishable ^{1}H NMR spectra obtained for **LutInam** and **LutInam2** polymorphs confirm their identical composition (Fig. S28 and S29, ESI†).

Raman spectroscopy. FT-Raman spectroscopy was applied to investigate changes in vibrational modes, related to intermolecular hydrogen bond interactions between flavonoids and coformers that occur upon their cocrystallization. Raman spectra for all of the discussed species and tentative assignments of vibrational modes based on studies conducted for individual cocrystal components[50–53] are given in Fig. S5–S14 and Tables S5–S8, ESI†) whereas spectra of cocrystals in the most characteristic region are presented in Fig. 10.

Formation of cocrystals results in significant changes in positions, intensities and shapes of bands in the 1700–1100 cm^{-1} region of the spectra. This enables discrimination between starting materials and resulting cocrystalline phases. In the 1750–1550 cm^{-1} region of the spectra of **FisNam**, **FisInam** and **GenNam**, the bands characteristic for cocrystal formation are mostly related to stretching vibrations of the C4=O group of flavonoids and amide I, amide II bands in Nam and Inam (Fig. 10a, b and e and Tables S5, S6 and S8, ESI†). There is also a simultaneous change in positions and shapes of bands related to bending vibrations of hydroxyl groups involved in intermolecular H-bonding. Additionally, in **FisNam** and **GenNam**, the band corresponding to the ρ_{NH2} vibration in

Nam is shifted to a higher wavenumber by 12 and 18 cm^{-1}, respectively. On the other hand, the amide III band in Nam and Inam is less affected by cocrystallization. Similar behavior is observed in the Raman spectra of two polymorphic forms of luteolin–isonicotinamide cocrystal when compared to the individual components (Fig. S6, S8, S12 and S13 and Table S7, ESI†).

Differences in intermolecular interactions and packing of both polymorphic forms **LutInam** and **LutInam2** are clearly reflected in different intensities, positions and shapes of bands in the region of 1700–1100 cm^{-1}. The most significant changes are observed for C–OH bending and C–O(H) stretching vibrations of luteolin as well as amide III band, stretching and bending vibrations of the pyridyl ring in isonicotinamide (Fig. 10c and d and Table S7, ESI†). In both forms of the cocrystal, typically for 5-hydroxyflavonoids, a strong intramolecular O5–H5···O4 hydrogen bond is observed. Analysis of interactions (motifs 8 and 12, Scheme 2) reveals that the O5 atom in **LutInam2** acts additionally as an acceptor of a N2A–H2A1···O5^{xvi} contact, what might account for different energies of vibrational modes related to C5–OH bending motions. These bands are centered at 1568 and 1502 cm^{-1} in **LutInam2** and shift to 1574 and 1507 cm^{-1} in **LutInam**. Moreover, differences in positions of peaks attributed to C13–OH and C14–OH bending vibrations in luteolin are presumably related to various hydrogen-bonding patterns (motifs 6 and 12, Scheme 2). Distinct signature peaks that enable discrimination between **LutInam** and **LutInam2** appear also in the low-frequency region below 400 cm^{-1}, which typically relates to lattice and phonon modes (Fig. S15, ESI†).

Thermal analysis. Thermal behavior of the five cocrystals was assessed by means of TG–DTA and DSC to provide insight into their phase transitions and thermal stability (plots are presented in the ESI,† Fig. S16–S25). Analysis of TG–DTA plots for **FisInam**, **LutInam** and **LutInam2** reveals no phase transitions and no significant weight loss before the melting event, with the latter observation confirming their unsolvated character. In **LutInam**, an endotherm is present as a first event in the DSC plot (onset temperature 245.1 °C, ΔH = 203.54 J g^{-1}, Fig. S23, ESI†), indicating its stability hitherto. The endotherm is followed by decomposition, accompanied by loss of isonicotinamide molecules (TGA: weight loss 30.7%, calculated 29.9%, Fig. S18, ESI†). DSC analysis of **FisInam** reveals a sharp endotherm (onset temperature 236.3 °C, ΔH = 163.47 J g^{-1}, Fig. S22, ESI†). Similar to **LutInam**, the event is followed by decomposition, with presumable loss of isonicotinamide molecules (TGA: weight loss 28.2%, calculated 29.9%, Fig. S17, ESI†). In **LutInam2**, a small weight loss ($\sim$1% in TGA, Fig. S19, ESI†) is observable in the range of 150–200 °C and might account for the presence of trace impurities. Upon further heating, a single endothermic event occurs (onset temperature 258.2 °C, ΔH = 292.16 J g^{-1}, Fig. S24, ESI†), and similar to previously described **FisInam** and **LutInam**, is correlated with decomposition and subsequent loss of isonicotinamide molecules (TGA: weight loss 27.3%, calculated 29.9%, Fig. S19, ESI†). In **FisNam**, the loss of ethanol molecules is observed in TGA, in the temperature range of 110–160 °C indicating gradual release (calculated weight loss is 4.2%, in agreement with experimental 4.7%, Fig. S16, ESI†). The event is seen by DSC as a broadened exotherm (onset temperature 141.6 °C, ΔH = 151.28 J g^{-1}, Fig. S21, ESI†). Desolvation is followed by decomposition upon further heating (a broad endotherm with an onset temperature of 190.3 °C, ΔH = 98.34 J g^{-1}) with a significant 41.3% weight loss determined by TGA, being in agreement with 44.0% calculated for stoichiometry of two nicotinamide molecules. Interestingly, the desolvation event does not lead to the immediate decomposition of the sample, confirming that ethanol molecules are not essential in sustaining the hydrogen-bonded network (see Crystal structure determination and characterization of cocrystals). Opposite behavior is observed for **GenNam**. Dehydration takes place gradually over the 80–115 °C range (TGA: calculated weight loss 4.4%, experimental 4.6%, Fig. S20, ESI†) and is seen by DSC as a broadened exotherm (onset temperature 89.3 °C, ΔH = 142.38 J g^{-1}, Fig. S25, ESI†). Decomposition of **GenNam** is subsequent to dehydration and leads to the release of nicotinamide molecules (TGA: weight loss 34.3%, calculated 29.8%). Such behaviour confirms the role of water molecules in sustaining 1D, 2D and 3D hydrogen-bonded arrangement of molecules within the cocrystal.

In summary, the unsolvated cocrystals (**FisInam**, **LutInam**, **LutInam2**) exhibit thermal stability up to a range of 230–260 °C (depending on the studied species), with decomposition temperatures in between that of melting points reported for pure flavonoids and the coformers (fisetin, 278 °C;[54] luteolin, 328 °C;[55] isonicotinamide, 155 °C[56]). Of the two solvated cocrystals, **GenNam** is the less stable (up to 80 °C, with subsequent dehydration and decomposition), whereas in **FisNam** desolvation begins at 110 °C, and the cocrystalline phase remains stable up to *ca.* 180 °C where it decomposes.

Conclusions

Three naturally-occurring polyphenolic compounds of pharmaceutical interest, namely fisetin, luteolin and genistein, were combined with nicotinamide and isonicotinamide with an aim to obtain their cocrystals. A screening experiment utilizing solvent drop grinding (SDG) method enabled identification of new cocrystalline phases, five of which, namely **FisInam**, **FisNam**, **LutInam**, **LutInam2** and **GenNam**, were successfully crystallized in SE experiment and characterized by single-crystal X-ray diffraction, FT-Raman spectroscopy, thermal analysis (DSC and TG–DTA) and ^{1}H NMR in solution. The results of the screening experiment reveal the importance of solvent selection as related to the amount of obtainable cocrystals, and call for employing a variety of solvents if the screening experiment is to provide vast results. Structural characterization of **FisNam**, **FisInam**, **LutInam**, **LutInam2** and **GenNam** cocrystals yields further information concerning supramolecular motifs in the little known field of flavonoid–coformer interactions. All of the reported compounds share a common supramolecular motif, being the O–H···N_{arom} interaction, in which the O7 hydroxyl functionality of flavonoid is engaged. Inspection of previously published quercetin–isonicotinamide (1 : 1)[11] and hesperetin–isonicotinamide (1 : 1)[27] cocrystals reveals that an isolated 7-hydroxyl moiety

acts as a donor in the O–H···N_{arom} motif in a universal manner. Those observations might be in correlation with the fact that the 7-hydroxyl substituent is the most acidic group in luteolin,[57] genistein[58] as well as quercetin,[59] hesperetin[60] and presumably fisetin. Comparative analysis of supramolecular motifs reveals that structural differences between flavonoid cocrystals are correlated with mutual orientations of flavonoids and coformer molecules, and are also attributed to the stoichiometry and presence of solvent in the crystal lattice. Two of the reported compounds (**FisNam** and **GenNam**) are cocrystal solvates, in which H-bonded interactions with solvent molecules are distinct. In **FisNam**, ethanol molecules act as donors for hydrogen bonding between their OH moieties and O3 and O4 functionalities of Fis, apart from which no other interactions are observed. Opposingly, in **GenNam**, water molecules are engaged in tri-fold hydrogen-bonded interactions. It is also noteworthy that we isolated and characterized for the first time two polymorphic forms of a flavonoid cocrystal, namely **LutInam** and **LutInam2**, with FT-Raman and DSC plots enabling their doubtless distinction. Thermal analyses reveal that the unsolvated **FisInam**, **LutInam** and **LutInam2** cocrystals are stable up to *ca.* 230, 250 and 260 °C, respectively. On the other hand, solvated **FisNam** and **GenNam** cocrystals exhibit loss of solvent molecules above 110 and 80 °C, respectively, and the desolvated **FisNam** cocrystal shows further stability up to 180 °C while decomposition of **GenNam** is subsequent to the release of water molecules. Finally, our results show that application of pyridinecarboxamide coformers is a successful approach towards the preparation of flavonoid cocrystals by both solvent drop grinding method and cocrystallization from solution.

Acknowledgements

Financial support by a statutory activity subsidy from the Polish Ministry of Science and Higher Education for the Department of Chemistry of Wroclaw University of Technology is gratefully acknowledged. We also gratefully acknowledge the instrumental grant 6221/IA/119/2012 from the Polish Ministry of Science and Higher Education, which supported our Integrated Laboratory of Research and Engineering of Advanced Materials where Raman measurements were performed.

References

1 C. G. Fraga, I. B. Jaganath and A. Crozier, Dietary flavonoids and phenolic compounds, in *Plant Phenolics and Human Health: Biochemistry, Nutrition, and Pharmacology*, ed. C. G. Fraga, John Wiley & Sons, Inc, 2010.
2 A. Crozier, I. B. Jaganath and M. N. Clifford, *Nat. Prod. Rep.*, 2009, **26**, 1001–1043.
3 M. R. Guzzo, M. Uemi, P. M. Donate, S. Nikolaou, A. E. Machado and L. T. Okano, *J. Phys. Chem. A*, 2006, **110**, 10545–10551.
4 N. Mignet, J. Seguin, M. Ramos Romano, L. Brullé, Y. S. Touil, D. Scherman, M. Bessodes and G. G. Chabot, *Int. J. Pharm.*, 2012, **423**, 69–76.
5 N. Qiao, M. Li, W. Schlindwein, N. Malek, A. Davies and G. Trappitt, *Int. J. Pharm.*, 2011, **419**, 1–11.
6 N. Shan and M. J. Zaworotko, *Drug Discovery Today*, 2011, **419**, 1–11.
7 Generally regarded as safe, a list is published by the U.S. Food and Drug Administration (FDA), http://www.fda.gov/Food/FoodIngredientsPackaging/GenerallyRecognizedasSafeGRAS/default.htm.
8 N. Bladgen, M. de Matas, P. T. Gavan and P. York, *Adv. Drug Delivery Rev.*, 2007, **59**, 617–630.
9 C. B. Aakeröy, S. Forbes and J. Desper, *J. Am. Chem. Soc.*, 2009, **131**, 17048–17049.
10 K. Shiraki, N. Takata, R. Takano, Y. Hayashi and K. Terada, *Pharm. Res.*, 2008, **25**, 2581–2592.
11 A. J. Smith, P. Kavuru, Ł. Wojtas, M. J. Zaworotko and R. D. Shytle, *Mol. Pharmaceutics*, 2011, **8**, 1867–1876.
12 O. L. Woodman and E. Ch. Chan, *Clin. Exp. Pharmacol. Physiol.*, 2004, **31**, 786–790.
13 K. Ishige, D. Schubert and Y. Sagara, *Free Radical Biol. Med.*, 2001, **30**, 433–446.
14 H. H. Park, S. Lee, J. M. Oh, M. S. Lee, K. H. Yoon, B. H. Park, J. W. Kim, H. Song and S. H. Kim, *Pharmacol. Res.*, 2007, **55**, 31–37.
15 M. Funakoshi-Tago, K. Nakamura, K. Tago, T. Mashino and T. Kasahara, *Int. Immunopharmacol.*, 2011, **11**, 1150–1159.
16 N. Khan, M. Asim, F. Afaq, M. Abu Zaid and H. Mukhtar, *Cancer Res.*, 2008, **68**, 8555–8563.
17 Y. S. Touil, J. Seguin, D. Scherman and G. G. Chabot, *Cancer Chemother. Pharmacol.*, 2010, **68**, 445–455.
18 M. López-Lázaro, *Mini-Rev. Med. Chem.*, 2009, **9**, 31–59.
19 C. P. Xavier, C. F. Lima, A. Preto, R. Seruca, M. Fernandes-Ferreira and C. Pereira-Wilson, *Cancer Lett.*, 2009, **281**, 162–170.
20 S. F. Yang, W. E. Yang, H. R. Chang, S. C. Chu and Y. S. Hsieh, *J. Dent. Res.*, 2008, **87**, 401–406.
21 S. Banerjee, Y. Li, Z. Wang and F. H. Sarkar, *Cancer Lett.*, 2008, **269**, 226–242.
22 N. J. Raynal, L. Momparler, M. Charbonneau and R. L. Momparler, *J. Nat. Prod.*, 2008, **71**, 3–7.
23 J. A. Bis, P. Vishweshwar, D. Weyna and M. J. Zaworotko, *Mol. Pharmaceutics*, 2007, **4**, 401–416.
24 F. H. Allen, *Acta Crystallogr., Sect. B: Struct. Sci.*, 2002, **B58**, 380–388.
25 (*a*) N. Schultheiss and A. Newman, *Cryst. Growth Des.*, 2009, **9**, 2950–2967; (*b*) A. Mukherjee, P. Grobelny, T. S. Thakur and G. R. Desiraju, *Cryst. Growth Des.*, 2011, **11**, 2637–2653; (*c*) R. Thakuria, S. Cherukuvada and A. Nangia, *Cryst. Growth Des.*, 2012, **12**, 3944–3953.
26 M. Sowa, K. Ślepokura and E. Matczak-Jon, *Acta Crystallogr., Sect. C: Cryst. Struct. Commun.*, 2012, **C68**, o262–o265.
27 P. Kavuru, *MSc thesis*, University of South Florida, USA, 2008, http://scholarcommons.usf.edu/etd/325.
28 Oxford Diffraction, *CrysAlis CCD and CrysAlis RED in Xcalibur PX and Kuma KM-4-CCD software*, Oxford Diffraction Ltd, Yarnton, Oxfordshire, England, 2009.
29 G. M. Sheldrick, *Acta Crystallogr., Sect. A: Found. Crystallogr.*, 2008, **A64**, 112–122.

30 W. Kraus and G. Nolze, *J. Appl. Crystallogr.*, 1996, **29**, 301–303.
31 K. Brandenburg, *DIAMOND*, Crystal Impact GbR, Bonn, Germany, 2005.
32 S. K. Wolff, D. J. Grimwood, J. J. McKinnon, M. J. Turner, D. Jayatilak and M. A. Spackman, *CrystalExplorer, version 3.0*, University of Western Australia, 2012.
33 P. J. Cox, Y. Kumarasamy, L. Nahar, S. D. Sarker and M. Shoeb, *Acta Crystallogr.*, 2003, **59**, o975.
34 T. Friščić and W. Jones, *Cryst. Growth Des.*, 2009, **9**, 1621–1637.
35 S. Karki, T. Friscić, W. Jones and W. D. Motherwell, *Mol. Pharmaceutics*, 2007, **4**, 347–354.
36 M. Arhangelskis, G. O. Lloyd and W. Jones, *CrystEngComm*, 2012, **14**, 5203–5208.
37 A. V. Trask, J. van de Streek, W. D. S. Motherwell and W. Jones, *Cryst. Growth Des.*, 2005, **5**, 2233–2241.
38 M. C. Etter, *Acc. Chem. Res.*, 1990, **23**, 120–126.
39 V. Sudhakar, T. N. Bhat and M. Vijayan, *Acta Crystallogr., Sect. B: Struct. Crystallogr. Cryst. Chem.*, 1980, **B36**, 125–128.
40 S. Domagala, P. Munshi, M. Ahmed, B. Guillot and C. Jelsch, *Acta Crystallogr., Sect. B: Struct. Sci.*, 2011, **B67**, 63–78.
41 Y. Miwa, T. Mizuno, K. Tsuchida, T. Taga and Y. Iwata, *Acta Crystallogr., Sect. B: Struct. Sci.*, 1999, **B55**, 78–84.
42 E. Molins, C. Miravitlles, J.-C. Wallet and E. M. Gaydou, *Acta Crystallogr., Sect. C: Cryst. Struct. Commun.*, 1996, **C52**, 925–929.
43 D. J. Timmons, M. R. Pacheco, K. A. Fricke and C. Slebodnick, *Cryst. Growth Des.*, 2008, **8**, 2765–2769.
44 H. D. Clarke, K. K. Arora, H. Bass, P. Kavuru, T. T. Ong, T. Pujari, L. Wojtas and M. J. Zaworotko, *Cryst. Growth Des.*, 2010, **10**, 2152–2167.
45 C. B. Aakeröy, A. M. Beatty, B. A. Helfrich and M. Nieuwenhuyzen, *Cryst. Growth Des.*, 2003, **3**, 159–165.
46 (*a*) W. W. Porter III, S. C. Elie and A. J. Matzger, *Cryst. Growth Des.*, 2008, **8**, 14–16; (*b*) N. Schultheiss, M. Roe and S. X. M. Boerrigter, *CrystEngComm*, 2011, **13**, 611–619; (*c*) P. Sanphui, N. J. Babu and A. Nangia, *Cryst. Growth Des.*, 2013, **13**, 2208–2219; (*d*) N. Schultheiss, S. Bethune and J. O. Henck, *CrystEngComm*, 2010, **12**, 2436–2442.
47 E. J. Yearley, E. A. Zhurova, V. V. Zhurov and A. A. Pinkerton, *J. Am. Chem. Soc.*, 2007, **129**, 15013–15021.
48 A. P. Mazurek, L. Kozerski, J. Sadlej, R. Kawecki, E. Bednarek, J. Sitowski, J. C. Dobrowolski, J. K. Maurin, K. Biniecki, J. Witowska, P. Fiedor and J. Pachecka, *J. Chem. Soc., Perkin Trans. 2*, 1998, 1223–1230.
49 G. Grynkiewicz, O. Zegrocka-Stendel, W. Pucko, J. Ramza, A. Koscielecka, W. Kolodziejski and K. Wozniak, *J. Mol. Struct.*, 2004, **694**, 121–129.
50 J. L. Castro, J. F. Arenas, M. R. Lopez-Ramirez, J. Soto and J. C. Otero, *J. Colloid Interface Sci.*, 2013, **396**, 95–100.
51 J. M. Dimitrić Marković, Z. S. Marković, D. Milenković and S. Jeremić, *Spectrochim. Acta, Part A*, 2011, **83**, 120–9.
52 A. Rygula, T. P. Wrobel, J. Szklarzewicz and M. Baranska, *Vib. Spectrosc.*, 2013, **64**, 21–26.
53 R. Sekina, E. G. Robertson and D. McNaughton, *Vib. Spectrosc.*, 2011, **57**, 306–314.
54 A. Hasan, A. Sadiq, A. Abbas, E. Mughal, K. M. Khan and M. Ali, *Nat. Prod. Res.*, 2010, **24**, 995–1003.
55 X. H. Han, S. S. Hong, J. S. Hwang, M. K. Lee, B. Y. Hwang and J. S. Ro, *Arch. Pharmacal Res.*, 2007, **30**, 13–17.
56 K. S. Eccles, C. J. Elcoate, A. R. Maguire and S. E. Lawrence, *Cryst. Growth Des.*, 2011, **11**, 4433–4439.
57 G. Favaro, C. Clementi, A. Romani and V. Vickackaite, *J. Fluoresc.*, 2007, **17**, 707–714.
58 J. Zielonka, J. Gębicki and G. Grynkiewicz, *Free Radical Biol. Med.*, 2003, **35**, 958–965.
59 M. Tungjai, W. Poompimon, C. Loetchutinat, S. Kothan, N. Dechsupa and S. Mankhetkorn, *Open Drug Delivery J.*, 2008, **2**, 10–19.
60 R. Srirangam and S. Majumdar, *Int. J. Pharm.*, 2010, **394**, 60–67.

